Journal of Thermal Analysis and Calorimetry, Vol. 60 (2000) 895–908

APPLICATION OF THE ŠESTÁK–BERGGREN EQUATION TO ORGANIC AND INORGANIC MATERIALS OF PRACTICAL INTEREST

A. K. Burnham

Lawrence Livermore National Laboratory, Livermore, CA 94551, USA

Abstract

Reactions that have an initial acceleratory period are common in both organic and inorganic systems. The Šesták–Berggren equation, $dx/dt = -kx^n(1-x)^m[-\ln(x)]^p$, with p set to zero (also called the extended Prout–Tompkins (PT) equation) is an excellent empirical kinetic law for many of these systems. In this work, it is shown to fit both isothermal and constant heating rate pyrolysis data for a well-preserved algal kerogen in a petroleum source rock and two synthetic polymers (polycarbonate and poly-ether-etherketone), dehydration of calcium oxalate monohydrate, decomposition of ammonium percholorate, and diffusive release of gas implanted in materials. Activation energies derived by non-linear regression to multiple experiments are consistent with those derived by simple isoconversional methods. Errors caused by misapplication of first-order kinetics to single-heating-rate data are discussed briefly.

Keywords: nucleation kinetics, Prout–Tompkins equation, sigmoidal kinetics, thermal decomposition kinetics

Introduction

Our arrival at a version of the Šesták–Berggren kinetic law [1] was an indirect one. Coming from the application world of fossil energy, most of the reactions we initially investigated were either pseudo-first-order reactions or more complex systems that could be approximated by a system of independent parallel first-order reactions [2, 3]. Later, however, we found geopolymers that had non-isothermal reaction profiles narrower than a first-order reaction and that had an acceleratory phase similar to that of linear polyolefins [4]. The literature for polymer decomposition kinetics was full of potential kinetic rate laws for various limits of initiation and branching [5], but we ultimately settled on what we eventually recognized as an extended PT model [6]. We did so prior to penetrating the extensive, complex, and often contradictory thermal analysis literature, for basically the same reason as Prout and Tompkins [7]: it seemed to have the correct functional form to fit our data.

The general form we chose was

$$dx/dt = -kx^n (1-qx)^m \quad (1)$$

1418–2874/2000/ $ 5.00

Akadémiai Kiadó, Budapest
Kluwer Academic Publishers, Dordrecht

where x is the fraction remaining (x=1–α in the conventional thermal analysis literature, where α is the fraction reacted). The parameter m was used explicitly because we wanted a functional form that would have a limit of a first-order reaction, if appropriate, during non-linear regression fitting to multiple reaction profiles, as had been our practice since the mid 1980s. The parameter q was added to account for a non-zero initial reaction rate, since both our analysis and application software numerically integrates the reaction rates to calculate extents of reaction.

At first, we held n=1 during this regression analysis, because all the kerogens we initially investigated had non-isothermal profiles with essentially the same shape as a first-order reaction; m affects the width, but not the shape, of a reaction profile at constant heating rate. Later we dealt with a broader range of materials, for which some had a profile skewed to high temperature, and the parameter n provided the means to fit those profiles. At about the same time, we uncovered the paper of Šesták and Berggren [1], which provided a stronger link between our empirical approach to Eq. (1) and the thermal analysis literature.

Unlike most workers, we measure chemical kinetic parameters to make predictions of reaction extents under conditions of practical interest, so we constantly test the ability of our kinetic models to extrapolate over wide time-temperature conditions. Such tests provide a reality check for the often-academic exercise of Arrhenius parameter derivation. This work found the Šesták–Berggren equation with p=0 (or either the extended Prout–Tompkins equation or n^{th}-order nucleation reaction, as we often call it) to be a very powerful tool for a wide range of organic and inorganic thermal decomposition reactions.

Avrami–Erofeev *vs.* extended Prout–Tompkins

Those attempting to model reactions variously known as nucleation, auto-catalytic, acceleratory, or sigmoidal historically faced two basic choices: the Prout–Tompkins model:

$$dx/dt = -kx(1-x) \tag{2}$$

or the Avrami–Erofeev model:

$$dx/dt = -m'kx[-\ln(x)]^{1-1/m'} \tag{3}$$

The Šesták–Berggren model:

$$dx/dt = -kx^n(1-x)^m[-\ln(x)]^p \tag{4}$$

contains both Eqs (2) and (3) as limits for various combinations of 0 and 1 for m, n, and p. Obviously, m'=1/(1–p). As a practical matter, we have found, in agreement with comments in the literature, that setting either m or p to zero gives very similar results. A few examples are shown in Fig. 1. Consequently, we have ordinarily set p=0 and used non-linear regression to determine optimal values of n and m. These parameters have allowed us to fit all experimental data to the precision we thought was appropriate for uses we envisioned.

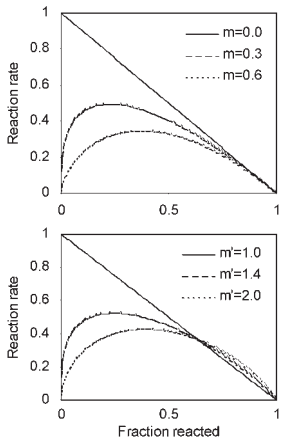

Fig. 1 Comparison of the extended PT (top) and Avrami–Erofeev (bottom) equations for parameter ranges typical of well-preserved kerogens and linear polyolefins

Extended Kissinger equation

The Kissinger equation [8] was originally derived for first-order reactions and shown to be exact for n^{th}-order reactions:

$$\ln(\beta/T_{max}^2) = -E/RT_{max} + \ln(AR/E) \tag{5}$$

where β is the heating rate. Chen, Gao, and Dollimore [9] subsequently showed that it holds more generally if the right hand term is replaced with $\ln(ARf'(\alpha)/E)$, where $f'(\alpha)$ is the derivative with respect to α, and $f(\alpha)$ is defined in

$$d\alpha/dt = kf(\alpha) \tag{6}$$

As long as T_{max} occurs at constant conversion, $f'(\alpha)$ is merely a constant that can be absorbed into the frequency factor. Even more generally, the Kissinger equation has been found both numerically [10] and analytically [11] to work well for systems of parallel reactions having a distribution of activation energies.

In anticipation of one new application of the Šesták–Berggren formalism presented here, the Kissinger equation also works for diffusive release upon heating of gas implanted at a specific initial depth in a material [12]. The evolution profile for that case is [13]

$$-\frac{dx}{dt} = \frac{c_0\delta}{2z^{3/2}(\pi D_0)^{1/2}}\exp(-E/RT)\exp\left(-\frac{\delta^2}{4D_0 z}\right) \tag{7}$$

where δ is the implantation depth, the diffusion constant is given by $D_0\exp(-E/RT)$, and z is the kinetic integral

$$z = \int_0^t \exp(-E/RT)dt \tag{8}$$

For a constant heating rate, differentiation of, and further manipulation of, Eq. (7) gives

$$\ln(\beta T_{max}^2) \approx -E/RT_{max} + \ln(2D_0/d^2E) \quad (9)$$

Several workers [4, 8, 10, 14], including Kissinger, have reported correlations between reaction order and the reaction profile shape at a constant heating rate. We previously reported correlations between the relative profile width (W_R–the ratio of the measured profile width to that calculated from approximate values of E and A derived from the Kissinger equation) and the width of the Gaussian distribution of energies in a parallel-reaction model. These correlations were used to provide initial guesses for a subsequent non-linear regression refinement of the kinetic parameters. Likewise, we developed similar correlations for m and n in Eq. (4) using profile width and asymmetry.

From the reaction rate profile at a constant heating rate, the value of n even for non-zero m can be estimated to within about 20% by the simple relationship

$$n_{asym} = (asym/0.64)^{0.78} \quad (10)$$

where $asym$ is the ratio $(T_{high}-T_{max})/T_{max}-T_{low})$ and T_{high} and T_{low} are the temperatures at which the profile crosses 25% of the maximum reaction rate. We have used different algorithms at various times to estimate the parameter m from the profile width. Kinetics98 v. 4.53 uses

$$m = W_R^{1.92}/n_{asym} \quad (11)$$

which works better for $n>2$ than the algorithm used earlier [16]. Also, we initially used $A_{PT} \approx A_{Kissinger}/(1-m)$ for materials having $m<0.5$, but this equation fails for m near 1. More recently, we have used

$$A_{PT} \approx A_{Kissinger}/(1-m+0.17m^2) \quad (12)$$

It must be emphasized that the purpose of these algorithms is to provide reasonable initial guesses for non-linear regression analysis, not to provide the ultimate in accuracy or rigor. Even so, they are far superior to the single heating-rate algorithms still used by some.

Examples

Oil generation

Our first application of a simplified version of the Šesták–Berggren equation, which we called a three-parameter model (A, E, and m), was for petroleum source rock kerogens [6]. The original sample for which we found both an acceleratory phase during isothermal pyrolysis in a fluidized bed and a narrow reaction profile is a partially mature algal source rock from the Uinta Basin, Utah (2557 m depth in the Brotherson 1-23B4 well) [4]. The reaction rate was measured by flame ionization detection of evolved hydrocarbons. Re-analysis of this sample was not reported in our first appli-

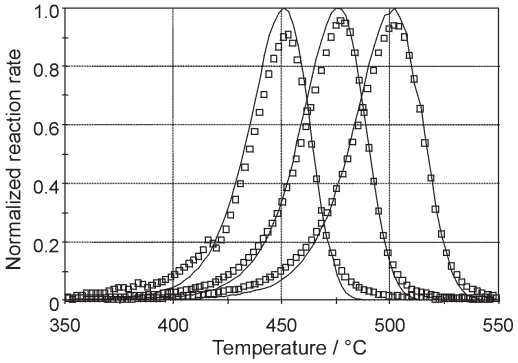

Fig. 2 Fit of the 3-parameter Prout–Tompkins model to hydrocarbon evolution from a well-preserved algal kerogen heated at 3.6, 14, and 50°C min^{-1}

cation of the '3-parameter' Prout–Tompkins equation to petroleum source rocks, so it is now reported in Table 1.

The half-width of the reaction profile is only 73% of that of a first-order reaction having an activation energy compatible with the shift in T_{max} with heating rate, but the profile asymmetry is about the same as a first-order reaction. Our simple correlations, denoted as extended Kissinger analysis, estimate a reaction order of 0.97 and a nucleation order of 0.44. Fixing n=1, a non-linear regression fit to the profile (Fig. 2) finds values of A and E very close to those of the extended Kissinger analysis. The fitted nucleation order is a little lower, due to the broader base of the reaction profile caused by volatilization of some extractable organic matter at low temperature and secondary char pyrolysis at the high temperature. As expected, the residual sum of squares of the non-linear regression parameters is substantially lower than that calculated

Table 1 Results for various kinetic analyses of a well-preserved kerogen from the Brotherson 1-23B4 well in the Unita Basin, Utah

Method	Standard Kissinger	Extended Kissinger	'3-parameter' NLR	Šesták–Berggren NLR	Single heating rate NLR
Average W_R		0.73			
Average *asym*		0.62			
A/s^{-1}	$1.49 \cdot 10^{14}$	$2.52 \cdot 10^{14}$	$2.61 \cdot 10^{14}$	$2.38 \cdot 10^{14}$	$6.32 \cdot 10^{18}$
E/kJ mol^{-1}	231.5	231.5	232.7	232.5	296.4
m	0	0.44	0.27	0.24	0
n	1	0.97	1	0.95	1
RSS of rates	5.39[a]	1.13[a]	0.207	0.202	1.59[a]
T_{max} (3°C/m.y.)	158°C	159	159	159	202

[a]Calculated for parameters fixed from independent analysis

from the Kissinger analysis parameters. Adding reaction order to the non-linear regression improves the quality of the fit very little.

In the last column of Table 1, parameters are given for fitting a first-order reaction to the middle section of the reaction profile. Freed from the constraints of the heating rate, A and E increase compensatingly to give a good fit to the single profile. However, when those parameters are used to calculate all three profiles, the agreement is no longer good in general, because T_{max} is overestimated for the slow heating rate and underestimated for the high heating rate. This demonstrates the futility of single-heating-rate fits for any predictive use. Also shown in the last row are the predicted temperatures for the maximum oil evolution rate at a geological heating rate. The single-heating-rate fit predicts oil generation at temperatures significantly higher than observed.

Polymer decomposition

The acceleratory or autocatalytic character of linear polymer pyrolysis was observed nearly 50 years ago [15]. The profile shapes of the nucleation models shown in Fig. 1 are very similar to those of random degradation and volatilization of high polymers. We previously showed [16] the ability of the extended Prout–Tompkins model to fit multiple-heating-rate, hydrocarbon-evolution curves of polyethylene, polydimethylenenaphthalene, polystyrene, polysulfone, and polyvinylacetate. A fit to similar data for polycarbonate is shown in Fig. 3. The extended Kissinger analysis gave E=209.4±6.0 kJ mol^{-1}, relative profile width of 0.50, and asymmetry of 0.70, yielding initial guesses of A=1.15·10^{12} s^{-1}, m=0.75, n=1.1 for the extended Prout–Tompkins model. The final non-linear regression parameters are given in the caption.

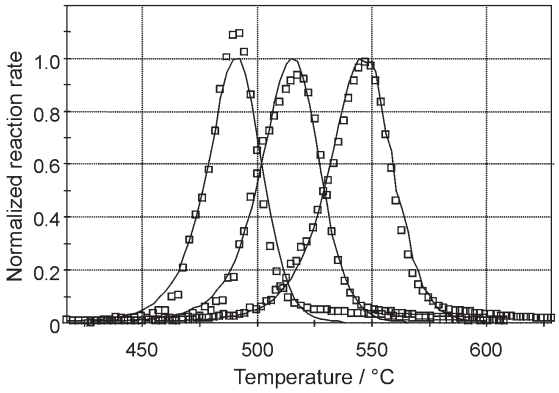

Fig. 3 Fit of the extended Prout–Tompkins model (Šesták–Berggren with p=0) to pyrolysis product evolution from polycarbonate heated at 5.3, 16, and 58°C min^{-1}. The NLR parameters are A=3.47·10^{12} s^{-1}, E=212.3 kJ mol^{-1}, m=0.69, and n=1.17

Another example of the power of the extended PT model comes from Nam and Seferis [17], who report both isothermal and non-isothermal TG measurements of polyether-ether-ketone (PEEK). After acknowledging the general functional form of

Eq. (1) with p=0, they derive a related equation for a sequence of a first-order, reversible dissociation reaction followed by a PT diffusive removal of products. They then provided a weighted sum of these two contributions to the observed reaction rate, yielding

$$-dx/dt=k[y_1x+y_2x(1-x)] \quad (13)$$

where y_1 and y_2 are the relative masses of chemical reaction and diffusion contributions to the overall rate and sum to one. While they analyze their data using an integrated form of Eq. (13), simple rearrangement shows

$$-dx/dt=kx(1-y_2x) \quad (14)$$

which equals Eq. (1) with n and m equal to one and $y_2=q$.

The TG data of Nam and Seferis for the main stage of PEEK decomposition were digitized and analyzed with Kinetics98 [18]. Kinetic parameters from the application of Eq. (1) are given in Table 2. The agreement is very good among our approximate extended Kissinger method for fractions reacted and non-linear regression analysis of non-isothermal, isothermal, and all data. The final column gives results for m, n, and q fixed to the values used by Nam and Seferis. The resulting A and E are close to both their values and our values obtained by finding optimal values of m, n, and q. A comparison of measured and calculated fractions reacted is given in Fig. 4. The agreement is excellent.

Table 2 Kinetic parameters from analysis of literature data for thermal decomposition of PEEK

Method	Extended Kissinger[a]	Constant HR only NLR	Isothermal only NLR	All data NLR	All data optimum q	All data: m, n, q fixed
Avg. W_R	0.36					
Avg. *asym*	0.62					
A/s^{-1}	$5.30\cdot10^{12}$	$4.74\cdot10^{12}$	$9.09\cdot10^{12}$	$2.38\cdot10^{14}$	$7.87\cdot10^{12}$	$8.91\cdot10^{12}$
E/kJ mol^{-1}	236.7	237.4	241.7	240.6	240.6	240.6
q		0.99	0.99	0.99	0.987	0.9785
m	1.00	0.44	0.87	0.86	0.90	1.00
n	0.45	0.97	0.92	0.89	0.92	1.00
RSS of α		$5.4\cdot10^{-3}$	$2.5\cdot10^{-2}$	$4.33\cdot10^{-2}$	$4.32\cdot10^{-2}$	$4.5\cdot10^{-2}$

[a]Based on correlations for W_R=relative $T_{80\%}-T_{20\%}$ and $asym=(T_{90\%}-T_{50\%})/(T_{50\%}-T_{10\%})$

The polycarbonate and PEEK examples emphasize two important points. The PEEK data show that the same kinetic model will usually work for isothermal and non-isothermal data over a similar wide range of time and temperature if the data is good and the kinetic analysis is done properly. Second, if improperly analyzed, erroneous kinetic parameters will result: if a single heating rate experiment is fitted to a first-order reaction, activation energies of 387 and 673 kJ mol^{-1} are obtained for poly-

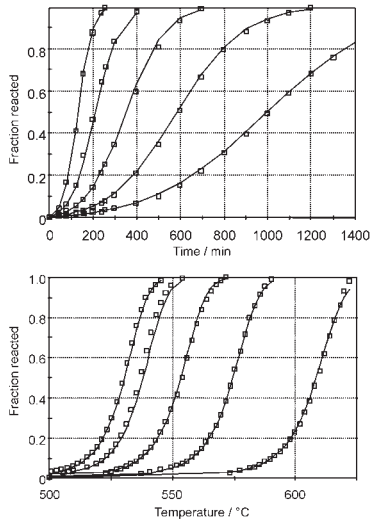

Fig. 4 Comparison of measured and calculated fractions reacted for decomposition of PEEK at both isothermal and constant heating rate conditions. The data were fit simultaneously, although they are shown separately for clarity

carbonate and PEEK, respectively, with correspondingly high frequency factors. The former energy is higher than expected for a chain reaction, and the latter is substantially higher than the strengths of C–C and C–O bonds. These high parameters are caused by forcing the *A–E* pair to compensate for the narrow reaction profile, instead of incorporating a parameter related to the acceleratory behavior. The effects of similar erroneous kinetic analyses are seen in high activation energies reported by some workers [19, 20] for thermal decomposition of cellulose and starch that were obtained by fitting a first-order reaction to a heating rate experiment. In contrast, the 3-parameter Prout–Tompkins model fits both multiple heating rate and isothermal experiments with activation energies similar to each other but significantly lower than from the single-heating-rate first-order fits [21].

Mineral dehydration

Calcium oxalate monohydrate is often used as a calibration standard for thermal analysis, but the literature contains substantial variation for both the temperatures and kinetic parameters for its decomposition [22 and references therein]. Christy *et al.* [22] report a careful study of the kinetics of the dehydration reaction by Fourier transform infrared spectrometry (FTIR). A particularly important result was that the dehydration reaction is not single step: there are two inequivalent crystal sites for the water, and they have different kinetics. Some of their data are reanalyzed here to obtain a better kinetic model.

Results from Friedman and extended Kissinger iso-conversional kinetic analysis of the disappearance of infrared absorbance bands for hydration water at 0.5 and 5°C min^{-1} are given in Tables 3 and 4. The activation energy is in the 90–110 kJ mol^{-1}

range, and the reaction profile is about 80% as wide as a first-order reaction and skewed slightly to low temperature relative to a first-order reaction. A superficial interpretation would be an n^{th}-order reaction, which would represent a receding interface model. However, Christy *et al.* showed that differentiation of the reaction profile revealed the clear presence of two overlapping reaction peaks, which is not consistent with a single n^{th}-order reaction. Instead, a fit of the fraction reacted data to two parallel nucleation reactions is more consistent with the spectroscopic data. The fit itself and the differentiated data are shown in Fig. 5, and the kinetic parameters are listed in Table 4. While this model is not definitive, because it does not consider the possible inter-conversion between the two sites, it does demonstrate that all previous kinetic analyses based on single-step models are inadequate.

Table 3 Friedman kinetic analysis of the dehydration reaction of calcium oxalate monohydrate as monitored by FTIR at 0.5 and 5°C min^{-1}

$1-x$	$\ln(Ax^n)$	$A(n=1)$	E/kJ mol^{-1}
0.1	24.65	$5.64\cdot10^{10}$	98.8
0.2	19.18	$2.68\cdot10^{8}$	82.4
0.3	23.66	$2.68\cdot10^{10}$	97.2
0.4	26.09	$3.55\cdot10^{11}$	105.3
0.5	23.50	$3.20\cdot10^{10}$	97.6
0.6	22.31	$1.22\cdot10^{10}$	93.7
0.7	25.65	$4.60\cdot10^{11}$	104.4
0.8	22.77	$3.87\cdot10^{10}$	95.6
0.9	19.00	$1.78\cdot10^{9}$	85.0

Table 4 Kinetic analysis by the extended Kissinger method and nonlinear regression to an n^{th}-order and parallel nucleation reaction models

Method	Extended Kissinger	n^{th}-order NLR	Parallel reaction	
			s #1(50%)	#2(50%)
Average W_R	0.79			
Average *asym*	0.63			
A/s^{-1}	$6.39\cdot10^{11}$	$5.11\cdot10^{10}$	$7.30\cdot10^{11}$	$1.39\cdot10^{11}$
E/kJ mol^{-1}	107.5	100.0	102.8	98.1
m	1.00	1.00	0.5	1.0
n	0.54	0.40	1.0	1.0
RSS of α		$7.0\cdot10^{2}$	$2.4\cdot10^{2}$	

Energetic materials

The decomposition of ammonium perchlorate has been studied extensively, and it is generally agreed that the decomposition has two stages: a sigmoidal decomposition

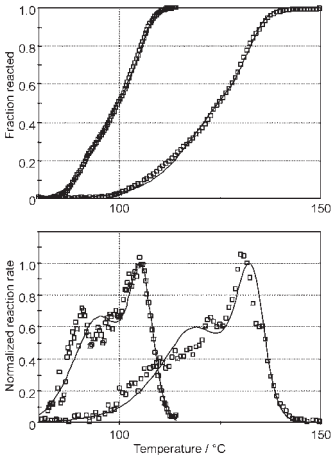

Fig. 5 Fit of the FTIR fraction reacted data for dehydration of calcium oxalate monohydrate at 0.5 and 5°C min^{-1} to two parallel nucleation reactions (top), and the differentiated data and calculated rates (bottom)

stage and a sublimation stage. Even so, there are still substantial variations in the reported kinetic parameters. Data for ammonium perchlorate decomposition were provided through the ICTAC kinetic analysis project [23].

The iso-conversional Friedman kinetic analysis, given in Table 5, provides an initial picture of the activation energy for this reaction. The trends found are very similar from isothermal and constant heating rate data, except that the isothermal data has an initial drop in the activation energy, in agreement with a similar analysis reported earlier by Vyazovkin and Wight [24]. During most of the first 30% of the reaction, the E is about 80 kJ mol^{-1}. During the last 70% of the reaction, the activation energy is about 115 kJ mol^{-1}. The preexponential factors are given for a qualitative indication, but they are not quantitatively valid due to the first-order approximation.

Table 5 Friedman-type isoconversional kinetic analysis of isothermal and non-isothermal decomposition of ammonium perchlorate

$1-x$	Isothermal data		Non-isothermal data	
	$A(n=1)$	E/kJ mol^{-1}	$A(n=1)$	E/kJ mol^{-1}
0.1	$8.9\cdot10^{6}$	107.3	$2.9\cdot10^{4}$	79.4
0.2	$4.9\cdot10^{4}$	83.9	$4.3\cdot10^{4}$	82.0
0.3	$1.5\cdot10^{3}$	71.8	$1.4\cdot10^{5}$	91.9
0.4	$8.7\cdot10^{7}$	124.5	$1.1\cdot10^{7}$	115.4
0.5	$8.2\cdot10^{7}$	123.6	$6.4\cdot10^{6}$	111.9
0.6	$2.8\cdot10^{7}$	117.8	$8.8\cdot10^{6}$	112.8
0.7	$2.1\cdot10^{7}$	115.1	$1.7\cdot10^{7}$	115.2
0.8	$6.2\cdot10^{8}$	128.8	$7.6\cdot10^{6}$	109.3
0.9	$8.7\cdot10^{6}$	107.4	$6.6\cdot10^{6}$	106.4

Table 6 Non-linear regression analysis of ammonium perchlorate decompostion data

Method	Extended Kissinger[a]		Isothermal data		Non-isothermal data	
	peak 1	peak 2	peak 1	peak 2	peak 1	peak 2
Average W_R	0.45	0.57				
Average *asym*	(high *T*)	(low *T*)				
A/s^{-1}	$3.2\cdot10^{7}$	$2.8\cdot10^{4}$	$2.96\cdot10^{4}$	$1.53\cdot10^{6}$	$1.97\cdot10^{7}$	$2.27\cdot10^{6}$
E/kJ mol^{-1}	98.8	116.0	68.9	107.0	95.5	108.3
Wt. frac.			0.24	0.76	0.25	0.75
q			0.995		0.995	
m	~1	~0	1.00	0.00	1.00	0.00
n	>1	<1	1.31	0.14	1.83	0.25
RSS of α			$2.23\cdot10^{-2}$		$3.15\cdot10^{-2}$	

[a]Only a partial extended Kissinger analysis (based on rates) is given because of the overlapping peaks

With these starting estimates, non-linear regression was used to fit a parallel-reaction model (n^{th}-order nucleation and n^{th}-order reactions) to both the isothermal and non-isothermal data. The results of these fits are shown in Table 6. Only a partial extended Kissinger analysis (based on rates) is given, because of the overlapping peaks. However, from a combination of the measured profile widths and the visual asymmetry, the first peak must be a nucleation reaction with $n>1$, and the second reaction is an n^{th}-order reaction with $n<1$ and m about zero. Consequently, m was fixed at 1.00 and 0.00, respectively, for the two reactions, for both the isothermal and non-isothermal fits. Preliminary analysis found a minimum at about q=0.995 for the non-isothermal reaction, so the final convergence used that value to determine the masses, along with A, E, and n for both reactions. Observed and calculated curves track each other within the width of conventional plotting symbols, for both the isothermal and non-isothermal data. [25]

A significant question is whether the two reactions are indeed concurrent or instead sequential. In fact, why are there two reactions in the first place? Boggs and Kraeutle [26] state that their photographs clearly show the effect of enhanced sublimation in vacuum, which occurred simultaneously with decomposition. This seems to support the concurrent reaction model, although the change in surface area during the reaction could change the relative proportions of decomposition and sublimation. Several authors [26–28] say the decomposition is catalyzed by impurities, and ultra-high-purity ammonium perchlorate shows only 9% disappearance via decomposition [26]. One possible explanation is that the catalytic impurities are gradually poisoned by the decomposition process, leaving only sublimation during the last portion of the reaction. The initial drop in activation energy for isothermal conditions might be explained by sublimation being dominant during the first portion of the reaction before the decomposition reaction gets going, although test calculations indicate that an initiation parameter of 0.999 or greater would be required. Alternatively, perhaps

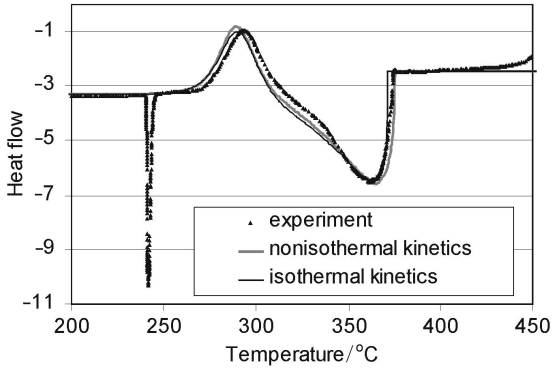

Fig. 6 Comparison of measured DSC data at °C min^{-1} with heat flow data calculated from the isothermal and non-isothermal TG kinetics. The spike at 241°C is an orthorhombic-cubic phase transition

the initial high activation energy for the isothermal case is due to a more dominate impact of the nucleation process.

Even though the mechanisms mentioned cannot be adequately tested with only mass loss data, the utility of the empirical kinetic model can be tested against DSC data kindly provided by Vyazovkin (Univ. of Utah). The two reactions were summed with the assumptions that the decomposition reaction is exothermic and that the evaporation reaction is endothermic. The baseline heat flow was assumed to be proportional to remaining mass. A comparison of the data with both the isothermal and non-isothermal kinetics is shown in Fig. 6. The non-isothermal calculation has been shifted up 5°C to match both the isothermal kinetics and the non-isothermal DSC curve. Perhaps this indicates a slight temperature calibration error in the non-isothermal TG data, since the isothermal TG and non-isothermal DSC data agree.

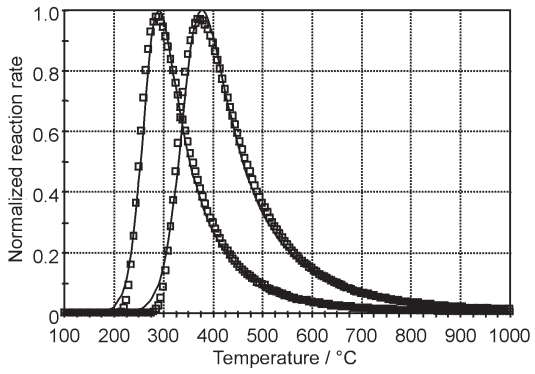

Fig. 7 Fit of synthetic data at 1 and 10°C min^{-1} for diffusive release of hydrogen from boron carbide to extended PT model

Diffusive release of implanted gas

First and n^{th}-order rate laws are frequently used to analyse temperature programmed desorption data, sometimes using data at only one heating rate [29]. In the case of implanted gas, this procedure would seem to be doubly risky, as there should be an induction time before the first gas reaches the surface. Equations (7)–(9) show that multiple heating-rate data can be treated by a Kissinger-type equation to obtain the preexponential factor and activation energy, but this still does not address the induction period issue.

We recently showed [12] that the extended PT formalism is one way to deal with this induction time. One example for synthetic data mimicking hydrogen implanted at a depth of 0.4 μm in boron carbide is shown in Fig. 7. The initiation parameter q was set at 0.999999, because little improvement occurred as q got closer to unity. Table 7 shows the results from this and other fits at other implantation depths, showing that apparent frequency factor does vary with the square of the implantation depth. The activation energy of 70 kJ mol^{-1}, used to create the synthetic data set, is recovered by the extended PT formalism.

Table 7 Non-linear regression parameters derived from fitting an extended PT model to synthetic diffusive evolution of hydrogen implanted in boron carbide at various depths

Parameter	0.2 μm	0.4 μm	0.6 μm
E/kJ mol^{-1}	70.2	70.2	70.0
A/s^{-1}	$9.6\cdot10^3$	$2.45\cdot10^3$	$1.065\cdot10^3$
Reaction order, n	3.64	3.69	3.73
Nucleation order, m	0.45	0.45	0.46

Conclusions

In the diverse set of examples presented here, both polymeric and inorganic, the Šesták–Berggren equation with p=0 works very well for correlating kinetic data over wide ranges of temperatures and pressures for reactions having sigmoidal reaction characteristics. Essentially the same rate parameters work well for isothermal and constant-heating-rate experiments. Consequently, it can be used with some confidence to extrapolate reaction rates outside the range of calibration. The Šesták–Berggren model also suggests some qualitative aspects of reaction mechanism, but one should be careful not to over interpret the meaning of the parameters without supplementary observations (e.g., microscopy, evolved gas analysis).

In contrast, a first-order reaction may fit data from a single heating rate well, but the activation energy for nucleation reactions will ordinarily be significantly higher than the true value, and the frequency factor will vary with the heating rate. Such kinetics are useful for neither extrapolation nor mechanistic interpretation and should not be considered acceptable practice.

This work was performed under the auspices of the U. S. Department of Energy by the Lawrence Livermore National Laboratory under contract no. W-7405-ENG-48. The DSC data for ammonium perchlorate was provided by S. Vyazovkin of the University of Utah.

References

1 J. Šesták and G. Berggren, Thermochim. Acta, 3 (1971) 1.
2 A. K. Burnham, R. L. Braun, H. R. Gregg and A. M. Samoun, Energy & Fuels, 1 (1987) 452.
3 A. K. Burnham, M. S. Oh, R. W. Crawford and A. M. Samoun, Energy & Fuels, 3 (1989) 42.
4 R. L. Braun, A. K. Burnham, J. G. Reynolds and J. E. Clarkson, Energy & Fuels, 5 (1991) 192.
5 H. H. G. Jellinek, Aspects of Degradation and Stabilization of Polymers, Elsevier, Amsterdam 1978.
6 A. K. Burnham, R. L. Braun, T. T. Coburn, E. I. Sandvik, D. J. Curry, B. J. Schmidt and R. A. Noble, Energy & Fuels, 10 (1996) 49.
7 E. G. Prout and F. C. Tompkins, Trans. Faraday Soc., 40 (1944) 488.
8 H. E. Kissinger, Anal. Chem., 29 (1957) 1702.
9 D. Chen, X. Gao and D. Dollimore, Thermochim. Acta, 215 (1993) 109.
10 R. L. Braun and A. K. Burnham, Energy & Fuels, 1 (1987) 153.
11 E. G. Seebauer, Surf. Sci., 316 (1994) 391.
12 A. K . Burnham and A. A. Grossman, submitted to Surface Science.
13 G. Carter, D. G. Armour and P. Bailey, Vacuum, 34 (1984) 801.
14 K. H. Van Heek and J. Juentgen, Ber. Bunsenges Physik. Chemie, 72 (1968) 1223.
15 Polymer Degradation Mechanisms, National Bureau of Standards Circular 525, U. S. Department of Commerce, 1953.
16 A. K. Burnham and R. L. Braun, Energy & Fuels, 13 (1999) 1.
17 J.-D. Nam and J. C. Seferis, J. Poly. Sci.: B. Poly. Phys., 30 (1992) 455.
18 Available for U.S. Government work at http://www.doe.gov/html/osti/estsc/estsc.html and for commercial purposes at http://www.humble-inc.com/indexhis.htm
19 G. Várhegyi, E. Jakob and M. J. Antal, Jr., Energy & Fuels, 8 (1994) 1345.
20 P. Aggarwal, D. Dollimore and H. Heon, J. Thermal Anal., 50 (1997) 7.
21 J. G. Reynolds and A. K. Burnham, Energy & Fuels, 11 (1997) 88.
22 A. A. Christy, E. Nodland, A. K. Burnham, O. M. Kvalheim, and B. Dahl, Appl. Spectroscopy, 48 (1994) 561.
23 M. E. Brown, Thermochim. Acta, 307 (1997) 201.
24 S. Vyazovkin and C. A. Wight, Intl. Rev. Phys. Chem., 17 (1998) 407.
25 A. K. Burnham, Thermochim. Acta, in press.
26 T. L. Boggs and K. J. Kraeutle, Combustion Sci. Technol., 1 (1969) 75.
27 P. W. M. Jacobs and A. Russell-Jones, AAIA Journal, 5 (1967) 829, and references therein.
28 P. W. M. Jacobs and W. L. Ng, J. Solid State Chem., 9 (1974) 315.
29 P. A. Redhead, Vacuum, 12 (1962) 203.